UCLA
UCLA Previously Published Works

Title

Pyrogenic iron: The missing link to high iron solubility in aerosols

Permalink

https://escholarship.org/uc/item/4x29x70s

Journal

Science Advances, 5(5)

ISSN

2375-2548

Authors

Ito, Akinori
Myriokefalitakis, Stelios
Kanakidou, Maria
et al.

Publication Date

2019-05-03

DOI

10.1126/sciadv.aau7671

Peer reviewed

ENVIRONMENTAL STUDIES

Pyrogenic iron: The missing link to high iron solubility in aerosols

Akinori Ito[1]*, Stelios Myriokefalitakis[2,3], Maria Kanakidou[4], Natalie M. Mahowald[5], Rachel A. Scanza[5], Douglas S. Hamilton[5], Alex R. Baker[6], Timothy Jickells[6], Manmohan Sarin[7], Srinivas Bikkina[7], Yuan Gao[8], Rachel U. Shelley[9], Clifton S. Buck[10], William M. Landing[9], Andrew R. Bowie[11], Morgane M. G. Perron[11], Cécile Guieu[12], Nicholas Meskhidze[13], Matthew S. Johnson[14], Yan Feng[15], Jasper F. Kok[16], Athanasios Nenes[3,17,18], Robert A. Duce[19]

Atmospheric deposition is a source of potentially bioavailable iron (Fe) and thus can partially control biological productivity in large parts of the ocean. However, the explanation of observed high aerosol Fe solubility compared to that in soil particles is still controversial, as several hypotheses have been proposed to explain this observation. Here, a statistical analysis of aerosol Fe solubility estimated from four models and observations compiled from multiple field campaigns suggests that pyrogenic aerosols are the main sources of aerosols with high Fe solubility at low concentration. Additionally, we find that field data over the Southern Ocean display a much wider range in aerosol Fe solubility compared to the models, which indicate an underestimation of labile Fe concentrations by a factor of 15. These findings suggest that pyrogenic Fe-containing aerosols are important sources of atmospheric bioavailable Fe to the open ocean and crucial for predicting anthropogenic perturbations to marine productivity.

INTRODUCTION

Marine primary productivity, nitrogen fixation, and particulate organic matter fluxes in the global open ocean are often controlled by the availability of the micronutrient iron (Fe) (1). Primary productivity is most sensitive to the amount of bioavailable Fe input in high-nutrient, low-chlorophyll regions, such as the sub-Arctic and equatorial Pacific, and the Southern Ocean. Atmospheric Fe-containing particles are important sources of bioavailable Fe to the ocean and can thus affect global climate via their influence on primary productivity (2). The solubility of Fe in ambient aerosols (i.e., the ratio of labile to total Fe) largely controls the bioavailability of this micronutrient after its deposition to the ocean (3–5). The term "labile" Fe in total Fe is operationally defined as the fraction of aerosol Fe that can be leached from the particulate phase into solution, in line with the widely held assumption that this form of Fe is readily bioavailable and therefore affects marine primary productivity (6).

Many factors can potentially affect aerosol Fe solubility near particle source regions and the subsequent enhancement of Fe solubility during atmospheric transport (7). Among these, atmospheric acidity is considered to be a key factor contributing to transformations of aerosol Fe from relatively insoluble to labile forms in the atmosphere (6). Notable progress has been made in our understanding of atmospheric inputs of labile Fe from natural and anthropogenic sources to the surface oceans (8). However, there are still large uncertainties regarding the relative importance of different sources of aerosol Fe and the effects of atmospheric processing on the solubility of the Fe delivered to the surface ocean. Furthermore, the experimental method for the determination of labile Fe in aerosols differs among research groups with regard to the leaching techniques used (e.g., batch versus flow-through), the leaching solutions and extraction times, and the analytical techniques (9). However, these differences do not appear to be the sole cause of the wide range of reported Fe solubilities (10). Generally, an increase in Fe solubility with a decrease in total aerosol Fe concentration appears to be a robust feature in global aerosol datasets (10, 11).

The natural emission of dimethylsulfide from the ocean surface and its oxidation to sulfuric acid was initially hypothesized to be linked to the photochemical transformation of Fe from mineral aerosols in the marine atmosphere (3). Further, the acid mobilization of Fe from mineral dust aerosols was also proposed via sulfuric acid formation from anthropogenic sources during long-range transport (7). The alternative hypothesis points to aerosol particle size as the driver for the enhancement of Fe solubility in dust-dominated aerosols (11), although this effect could not be reproduced in a subsequent study (12).

Atmospheric chemical transport models have considered the dissolution rates for mineral dust from laboratory experiments as a kinetic process, which is dependent on the pH, the mineral composition of Fe-containing particles, organic species (as Fe-reducing agents), and solar radiation (4, 13–15). The Fe dissolution scheme was improved on the basis of laboratory studies considering the types of Fe species associated with mineral dust source materials (16–20). Following these studies, three Fe pools were characterized as follows: labile Fe (e.g., ferrihydrite

[1]Yokohama Institute for Earth Sciences, JAMSTEC, Yokohama, Kanagawa 236-0001, Japan. [2]Institute for Marine and Atmospheric Research (IMAU), Utrecht University, 3584 CC Utrecht, Netherlands. [3]Institute for Environmental Research and Sustainable Development, National Observatory of Athens (NOA), GR-15236 Palea Penteli, Greece. [4]Environmental Chemical Processes Laboratory (ECPL), Department of Chemistry, University of Crete, 70013 Heraklion, Greece. [5]Department of Earth and Atmospheric Sciences, Cornell University, Ithaca, NY 14853, USA. [6]Centre for Ocean and Atmospheric Sciences, School of Environmental Sciences, University of East Anglia, Norwich, UK. [7]Physical Research Laboratory, Ahmedabad, India. [8]Rutgers University, Newark, NJ 07102, USA. [9]Florida State University, Tallahassee, FL 32301, USA. [10]Skidaway Institute of Oceanography, University of Georgia, Savannah, GA 31411, USA. [11]Institute for Marine and Antarctic Studies, University of Tasmania, Hobart, Tasmania, Australia. [12]Sorbonne Université, CNRS, Laboratoire d'Océanographie de Villefranche, LOV, F-06230 Villefranche-sur-mer, France. [13]North Carolina State University, Raleigh, NC 27695, USA. [14]NASA Ames Research Center, Moffett Field, CA 94035, USA. [15]Argonne National Laboratory, Argonne, IL 60439, USA. [16]Department of Atmospheric and Oceanic Sciences, University of California, Los Angeles, Los Angeles, CA 90095, USA. [17]Laboratory of Atmospheric Processes and Their Impacts, School of Architecture, Civil and Environmental Engineering, École Polytechnique Fédérale de Lausanne, Lausanne CH-1015, Switzerland. [18]Institute of Chemical Engineering Sciences, Foundation for Research and Technology Hellas, GR-26504 Patras, Greece. [19]Departments of Oceanography and Atmospheric Sciences, Texas A&M University, College Station, TX 77843, USA.
*Corresponding author. Email: akinorii@jamstec.go.jp

and nanosized Fe oxides), less labile Fe (e.g., heterogeneous inclusion of nano-Fe grains in aluminosilicates), and refractory Fe (e.g., crystalline and micrometer-sized iron oxides). The labile Fe fraction in aerosols is regarded as the most readily bioavailable form of Fe and often used as the input from atmospheric models to ocean biogeochemistry models. The fraction of less labile Fe in aerosols may be regarded as potentially bioavailable forms that can be photochemically transformed to labile forms in the atmosphere or after deposition into the ocean. "Less labile Fe" may be operationally distinguished from "labile Fe" by using specific leaching agents (21–23), which do not access the refractory Fe fraction (22, 23). Therefore, the labile and less labile content in aerosols may set the upper and lower limits for aerosol Fe solubility, respectively, as it applies to the marine environment.

Elevated levels of Fe solubility (>10%) have been observed in aerosols dominated by combustion sources (24–26). The physical and chemical properties of Fe oxides in combustion aerosols (e.g., coal fly ashes) are different from those of naturally occurring minerals due to combustion (27, 28). For instance, ferric sulfate and aggregated nano-crystals of magnetite (Fe_3O_4) are dominant components of Fe in oil fly ash (29, 30), formed via high-temperature combustion (>800°C) followed by sulfuric acid condensation and potentially modified by filtration of particles from the stack gas, depending on what emission controls are in place (31). Laboratory experiments suggested that Fe in coal fly ash could be mainly labile because of chemical transformations during acidic processing (27). The enhanced Fe solubility of combustion-derived aerosols has been incorporated into the atmospheric Fe transport models in two different ways (32, 33). One of the atmospheric chemical transport models discussed here has adopted a higher initial solubility for Fe sulfate derived from laboratory experiments on oil fly ashes only, and faster dissolution rates for all combustion aerosols, compared to mineral dust (33). Other models only assume higher initial solubilities in combustion aerosols including the oil fly ashes (18, 32).

Given the key role of Fe in ocean biogeochemistry (1) and the importance of atmospheric transport in delivering Fe to the remote oceans, it is critical to develop atmospheric Fe transport models that can realistically simulate total and labile Fe deposition fluxes to the oceans. These models can then provide a tool to consider how Fe deposition fluxes may have changed in the past and/or could change in the future and how anthropogenic perturbations might affect ocean biogeochemistry. Our companion article described four atmospheric Fe models, which participated in the Joint Group of Experts on the Scientific Aspects of Marine Environmental Protection (GESAMP) intercomparison study, and analyzed the differences in atmospheric concentrations and deposition fluxes between models, as well as between models and observations compiled from multiple field campaigns (34). The four models parameterize natural and anthropogenic Fe sources, atmospheric processing, and deposition differently (15, 18, 19, 28). We pointed out that the comparison of monthly mean model results with the shorter-term (e.g., daily) observations during different sampling periods introduced inaccuracies because of the variable nature of high aerosol Fe solubility.

Here, we performed a statistical analysis using the maximum likelihood method to compare Fe solubility between field data and model information (see Materials and Methods). We show better agreement in Fe solubility between model estimates and field data when higher solubility is simulated in pyrogenic Fe than lithogenic Fe for the global ocean and four separate oceanic regions from more to less air polluted conditions. We conclude that high Fe solubility in aerosols is mainly attributed to labile Fe released from pyrogenic Fe oxides. The description of the models and details of the statistical approach are provided in Materials and Methods.

RESULTS AND DISCUSSION

Comparison of simulated Fe solubility to field data over the global ocean

We compiled data for total and labile aerosol Fe concentrations simulated by four models (see Materials and Methods) and from digestions and leaches of aerosol samples collected during multiple field campaigns to improve our understanding of the factors controlling solubility (fig. S1 and tables S1 and S2). We used these data to assess the variability in the solubility of aerosol Fe using a diverse range of methodologies. To reduce the uncertainties associated with source attribution, some simulated data, for which maximum likelihood estimates (MLEs) of total Fe concentrations do not fall within $\pm 2\sigma_o$ of the measurements, are not used for the comparison with field data, as is described in Materials and Methods (fig. S2 and table S2). Here, σ_o represents the SD of Fe concentration for measurements. This procedure can eliminate the cases that result in a good agreement in labile Fe concentration by compensating the underestimates in Fe solubility with the overestimates in Fe concentration and vice versa, which would bias the relative contribution of combustion and mineral dust sources of Fe to labile Fe. Because direct association of model estimates to a specific cruise track and time period can introduce biases when used as a reference for larger regions and different time periods, the maximum likelihood method was implemented to estimate the state of the atmosphere from observations and models.

The ordinary arithmetic averages of simulated Fe solubility and weighted arithmetic averages of Fe solubility by simulated Fe concentration from the models are compared with the field data in table S3. The weighted mean values are calculated from the cumulated values of labile Fe and total Fe for all data points. The minimum (Min), maximum (Max), number of data points, mean error (Error), root mean square errors (RMSE), mean bias (Bias), and correlation coefficient (r) of Fe solubility between the model results and field data are also listed in table S3. The field data show a wider variability in Fe solubility compared to those in simulated Fe solubility under different conditions, ranging from the minimum (0.02%) to the maximum (98%) with an SD of 8.2 for the arithmetic averages. For each model, the arithmetic average of Fe solubility weighted by the total Fe concentration for all grid points with available observations, and its SD are lower than the corresponding ordinary arithmetic average of the Fe solubilities for the same grid points. This reflects the fact that high Fe concentrations with low solubilities near mineral dust source regions contribute more to the Fe concentrations than others such as combustion aerosols and aged mineral dust aerosols that are sampled over remote regions. The ratios of arithmetic averages to weighted averages for the field data (5.0) and the ratios of their SDs (104) are more consistent with those of the Integrated Massively Parallel Atmospheric Chemical Transport (IMPACT) model when considering both combustion aerosols and mineral dust (5.1 and 115) than those with mineral dust only (1.9 and 40) (table S3). Moreover, better agreement of the model results with the field data of labile Fe concentrations can be seen for IMPACT when considering combustion aerosols plus mineral dust than with mineral dust only (fig. S3 versus fig. S4). At the same time, IMPACT output fits the field data best (correlation

coefficient of 0.38 summarized in table S3) and also has the highest solubility estimates for combustion aerosols. This suggests that enhanced and more variable aerosol Fe solubility is associated with mixing of combustion aerosols and its atmospheric processing during transport.

The high Fe solubility (>10%) at low Fe concentration in the data was successfully simulated only by the IMPACT model (Fig. 1). The IMPACT model results suggest that combustion aerosols substantially contribute to labile Fe concentrations (>90%, red color in Fig. 1 and fig. S5). These results support the argument that the source-dependent composition of aerosols is an important factor in controlling the sporadically high Fe solubility (>10%) (25, 29, 35) under polluted conditions in the Northern Hemisphere. On the other hand, the Tracer Model 4 of the Environmental Chemical Processes Laboratory (TM4-ECPL) model assigned high Fe solubility to combustion aerosols but does not simulate high solubility at low concentrations in Fig. 1, mainly because of faster deposition rates for labile Fe than those for total Fe from combustion sources and the absence of the Fe dissolution process for combustion aerosols in TM4-ECPL. Moreover, the IMPACT model prescribed lower initial Fe solubility but simulated high solubility at low concentrations due to Fe released from Fe-containing combustion aerosols during transport. These results suggest that agreements with field data depend not only on the source chemical composition but also on the atmospheric processing during transport. The apparent deviation of Fe solubility in IMPACT from the 1-to-1 ratio is possibly due to the prescribed Fe solubility at emission by the arithmetic mean of field data

for oil fly ashes (58 ± 22%) (fig. S5) (29, 30, 36). In addition to the wide range in the initial Fe solubility for oil fly ashes, the Fe dissolution rates for combustion aerosols significantly vary between different samples used for laboratory experiments (27, 30). This suggests that IMPACT may need to resolve the actual variability in the degree of aerosol Fe lability at emission and in the subsequent atmospheric processes to better represent the aerosol source characteristics.

Iron solubility over the northern Indian Ocean

Observations from the northern Indian Ocean provide a valuable dataset to evaluate model performance, as Fe solubilities in aerosols sampled over the Bay of Bengal are considerably higher than those sampled over the neighboring Arabian Sea (Fig. 2 and fig. S1) (26, 37). The Fe solubility correlates linearly with the concentration of acidic species over the Indo-Gangetic Plain, suggesting that acid processing of Fe-containing aerosols influences Fe solubility during long-range transport (38). Moreover, enhanced levels of Fe solubility have been observed in aerosols dominated by biomass burning and fossil fuel combustion sources over the Bay of Bengal (38). IMPACT, TM4-ECPL, and the Community Atmosphere Model version 4 (CAM4), all of which include combustion aerosols, show to some extent the contrast between high Fe solubility in the Bay of Bengal and low solubility in the Arabian Sea, while the Goddard Earth Observing System with Chemistry (GEOS-Chem) model, which does not include combustion aerosols, shows lower Fe solubility over the Bay of Bengal. However, there are large differences regarding the relative importance of different sources of labile Fe (Fig. 2), due to differences in the relative source strength of dust and combustion Fe, and in solubility estimates for dust and combustion aerosols in the models. All models overestimate the low values of the Fe solubility in field data over the Arabian Sea by more than a factor of 10. This is primarily due to the prescribed solubility of labile Fe for dust aerosols in the models at their primary emissions and the subsequent enhancement of Fe solubility estimated from the simulated amount of atmospheric processing during transport in the models. We note that the low solubilities of the field data are outliers (triangles in fig. S5) in the modeled Fe solubility versus the field data. The Fe solubility from the field data used in this study (0.08 ± 0.09%) is significantly lower than those reported by other research groups over the Arabian Sea [1.4 ± 0.5% (39) and 0.4 ± 1.0% (40)]. These differences in the Fe solubility between investigators presumably reflect methodological and analytical differences in the measurements; these uncertainties could potentially be resolved if standard methods and reference material analysis were used by different investigators.

Iron solubility over the North Atlantic Ocean

The large body of available field data on aerosol Fe over the North Atlantic offers another useful area in which to compare the models. Air mass back trajectories (AMBTs) were used to classify the source regions and transport pathways for the aerosol samples collected over the North Atlantic (23, 41). However, AMBTs were not sufficiently discriminating to identify the aerosol sources or the potential effects of atmospheric processing on Fe solubility (23). In Fig. 3, the aerosol samples are classified as sourced by air masses from North Africa or other air mass regimes (23). The "degree of atmospheric processing" from the field data can be derived from the ratio of Fe solubility derived from two different leaching methods (see Materials and Methods) (21–23). All models calculate that mineral dust was the major source of labile Fe at high total Fe concentrations for samples largely influenced by North African air masses and reproduced the low solubility of 0.4 ± 0.1%

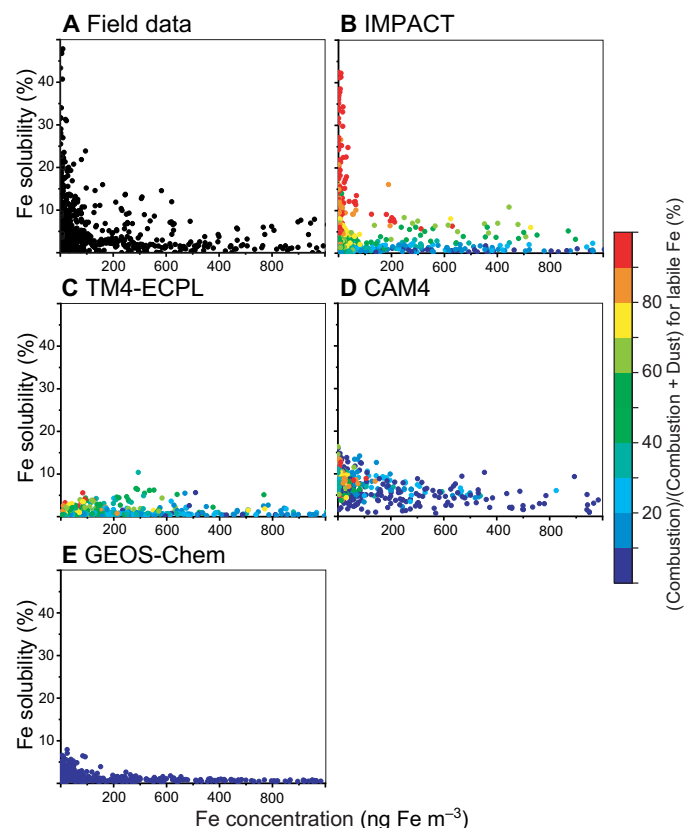**Fig. 1. Atmospheric concentration of total aerosol Fe (ng m⁻³) versus Fe solubility (%) for simulated estimates (colored circles) and field data (black circles).** (**A** to **E**) The color represents the (combustion)/(combustion + dust) ratio for labile Fe concentration in aerosols.
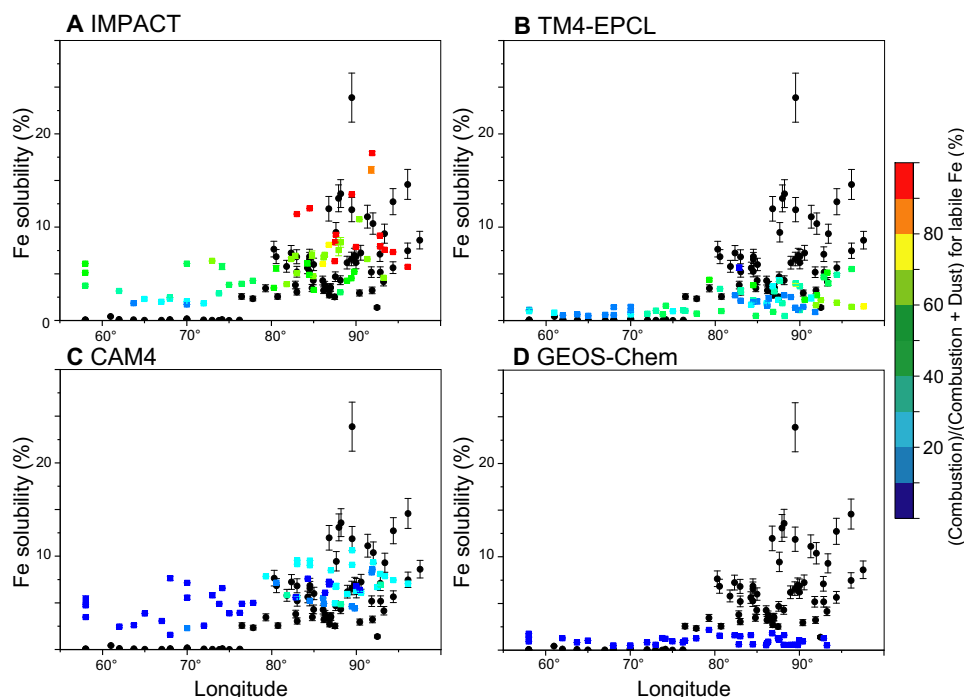
Fig. 2. Comparison of simulated atmospheric Fe solubility with field data (black circles) over the Bay of Bengal and Arabian Sea. (**A** to **D**) The color represents the simulated (combustion)/(combustion + dust) ratio (percent) for labile Fe concentration in aerosols.

of the field data. The internal mixing of alkaline components in mineral dust with Fe-containing minerals can lead to higher pH and thus suppression of Fe dissolution (4, 14, 18). In North African mineral dust aerosols, the ratio of labile Fe to the sum of labile and less labile Fe concentrations indicates a weak degree of Fe processing in aerosols (5.6 ± 2.2% on average from Eq. 3 in Materials and Methods). By contrast, non–North African air mass has a strong degree of Fe processing in aerosols (36 ± 15% on average). At the same time, the three models (IMPACT, TM4-ECPL, and CAM4) estimate a large contribution of combustion aerosols to the labile aerosol Fe at higher Fe solubility and lower aerosol Fe concentrations (Fig. 3). Moreover, IMPACT reproduced the sporadically high Fe solubility observed in aerosols from the other air mass regimes, specifically marine and high-latitude air masses.

Iron solubility over the equatorial Atlantic Ocean

The simulated Fe solubility is further compared with the field data (black symbols) in the equatorial Atlantic (Fig. 4). The atmospheric residence time, and thus the time available for atmospheric processing, of North African mineral dust aerosols increases as the dust is transported to the west, but there is no significant trend in Fe solubility for the field data with longitude, around 10°N across the tropical Atlantic (42). This low solubility of 2.0 ± 1.5% with no longitudinal trend for aerosol Fe is captured by IMPACT, TM4-ECPL, and GEOS-Chem.

Iron solubility over the Southern Ocean

Observations of Fe solubility near coastal areas may be affected by regional anthropogenic emissions, whereas those over the remote ocean may be influenced more by atmospheric processing during long-range transport. Over the Southern Ocean (Fig. 5), none of the models was able to reproduce the high Fe solubility (>10%) occasionally reported for aerosols (12 of 42 samples), because there is no aerosol Fe dissolution

mechanism under high-pH and low-oxalate conditions in IMPACT, TM4-ECPL, and GEOS-Chem. Additionally, the high Fe solubility of the field data in the Southern Ocean exceeds the sum of labile and less labile solubility (6.0 ± 1.0%) for North African dust (23) and the Fe solubility in glacial weathering products (2 to 3%) (29). Thus, such a wide range of solubility (from 0.2 to 48%) in this region as derived from observations cannot be explained by considering only chemical aging of mineral dust aerosol as measured in the laboratory. Different types of Fe-containing minerals such as pyrogenic Fe oxides must be considered in conjunction with additional aerosol processing such as plume chemistry to achieve these high solubilities. Moreover, averaged labile Fe concentration from all modeled estimates (0.065 ± 0.078 ng m^{-3}) underestimates the observed mean over the Southern Ocean (0.967 ± 1.049 ng m^{-3}) by a factor of 15.

We therefore suggest some mechanisms to explain these high solubilities. Pyrogenic Fe, which can be transformed to labile Fe during atmospheric processing, may play an important role in providing labile Fe to the Southern Ocean. However, further studies are required to identify and quantify such aerosol sources in the Southern Hemisphere (43–45). The higher solubility may originate from aerosol interactions with emissions from open biomass burning, which is common in the Southern Hemisphere (43, 44). Additionally, continental Fe-containing aerosols have longer lifetimes over remote oceanic regions in the Southern Hemisphere, such as in the outflow of South America, southern Africa, and Australia (34). Thus, aerosols originating from land can experience atmospheric processing over longer periods than in the Northern Hemisphere. An additional possibility is that some Fe dissolution processes may be missing from the models. For instance, dissolution of nanosized colloidal Fe oxides in ice is not taken into account in our models (46). Mineral dust in Antarctica snow samples was shown to have low Fe solubility (~0.7%) (47), which was consistent with the IMPACT model estimates, while the
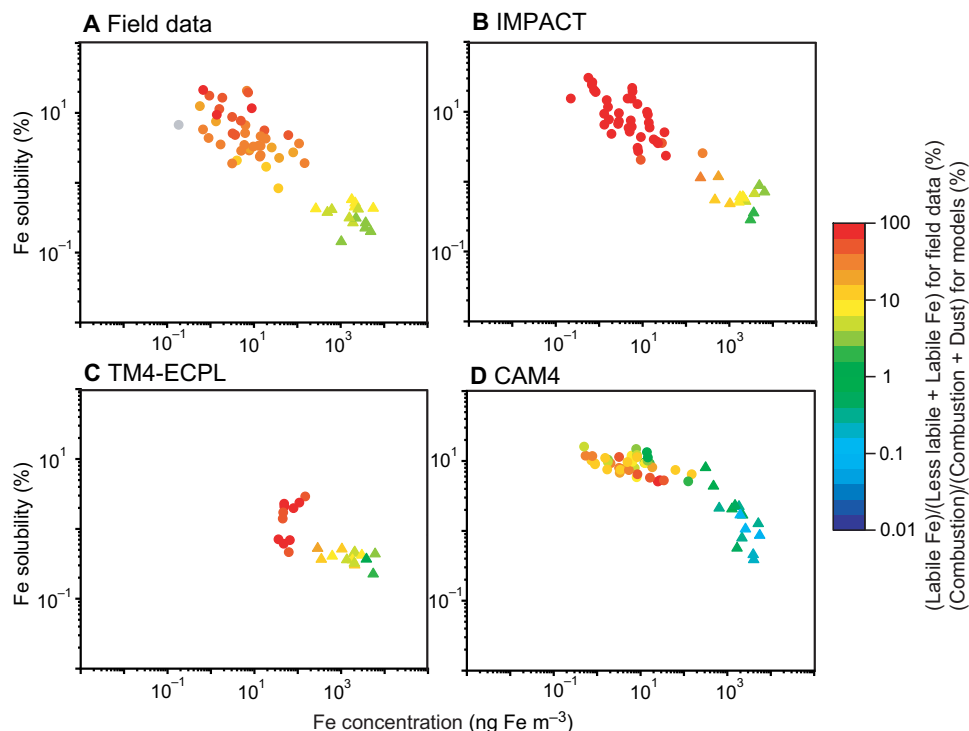
Fig. 3. Fe solubility versus Fe concentration (ng m⁻³) for field data and models over the North Atlantic. The colors for field data (**A**) represent percentage contributions of labile Fe to the sum of less labile and labile Fe concentrations in aerosols. The colors for the models (**B** to **D**) represent the simulated contribution of combustion aerosols to the sum of combustion and dust aerosols to labile Fe. The field data in light gray color represent no data for the 25% acetic acid leach. The aerosol samples are classified as sourced by two different air masses from North Africa (triangles) or other air mass regimes (circles) including North America, Europe, marine (no interaction with major land masses within 5 days before sample collection), or high latitudes (air masses originating north of 50°N) (*23*).
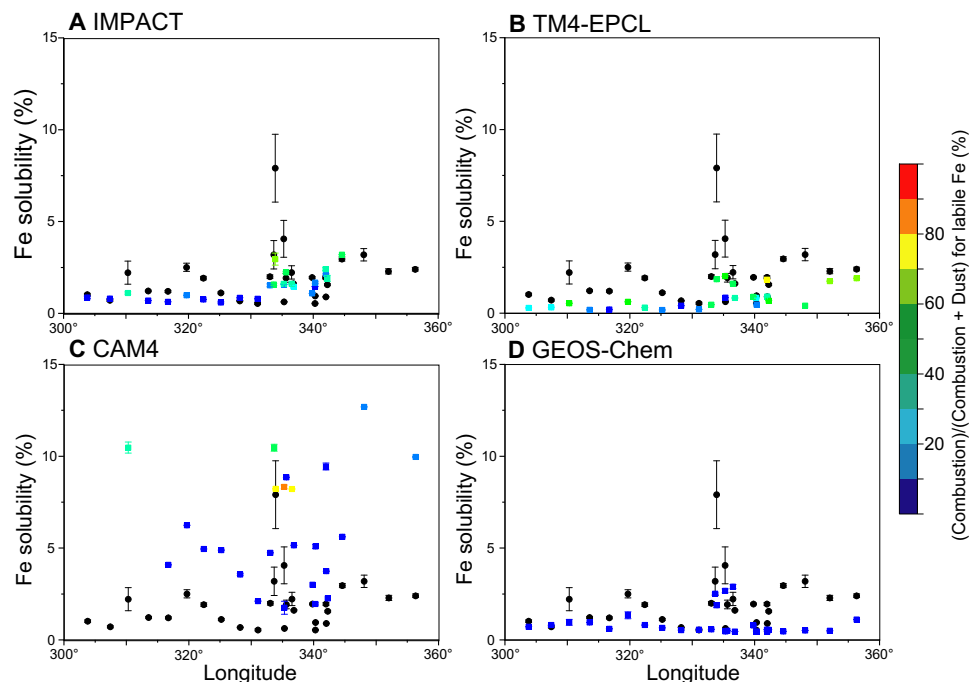
Fig. 4. Comparison of simulated atmospheric Fe solubility (colored points) with field data (black points) over the equatorial Atlantic. (**A** to **D**) The color represents the simulated (combustion)/(combustion + dust) ratio (percent) for labile Fe concentration in aerosols.
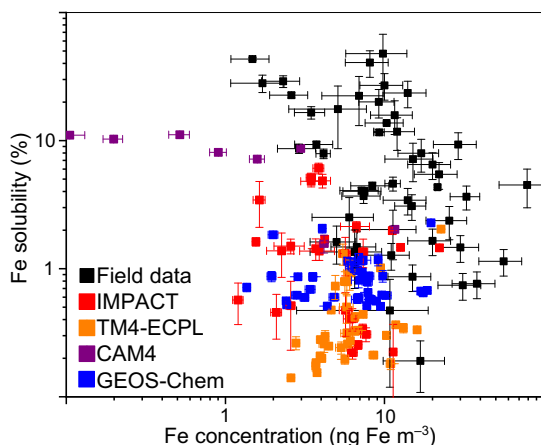
Fig. 5. Fe solubility versus Fe concentration (ng m^{-3}) for field data (black squares), IMPACT (red squares), TM4-ECPL (orange squares), CAM4 (purple squares), and GEOS-Chem (blue squares) over the Southern Ocean (>45°S). The vertical lines in symbols correspond to ±1 SD for Fe solubility in aerosols.

Fe-containing aerosols affected by fires may be associated with sporadic high Fe solubility (44). Thus, we recommend ice-enhanced dissolution experiments of representative combustion aerosols (e.g., biomass burning aerosols and volcanic ashes) under conditions relevant to ice particles in the atmosphere over the Southern Ocean. Studies of stable Fe isotopes may offer additional constraints on the contribution from combustion sources to aerosol Fe (48).

Uncertainty in aerosol Fe solubility stems from the scarcity of observations in the Southern Hemisphere. There are fewer field data in the Southern Hemisphere, which are sparsely distributed and collected over longer sampling periods during research cruises, partly due to low concentration of aerosols. Thus, these results should be interpreted with a degree of caution. We suggest that more observations are needed before drawing any firm conclusions on the Fe solubility and the models' performance in the Pacific, Indian, and Southern oceans. The high solubility in regions of low Fe concentration (<100 ng m^{-3}) was thought to be a robust feature of all the available data regardless of the leaching methods. However, low Fe solubilities were also found at low Fe concentrations over the Southern Ocean (Fig. 5) in some recent field data (10, 43, 49, 50). Given the key role of the Southern Ocean in the Earth system, it is important to gain a better understanding of pyrogenic and lithogenic Fe sources in the region alongside improved understanding of atmospheric processing of Fe-containing aerosols to resolve these discrepancies between model estimates and field data.

Simulated contribution of combustion aerosols to labile Fe
The contribution of combustion aerosols to total Fe deposition flux to the ocean, as calculated by the Fe deposition fluxes originating from dust and combustion sources (figs. S6 and S7), is shown in Fig. 6. Three models (IMPACT, TM4-ECPL, and CAM4) can calculate the contribution from combustion aerosols to total Fe and to labile Fe deposition fluxes. The models agree that mineral dust is the major source of Fe deposited to the North Atlantic, Arabian Sea, and South Atlantic downwind of the arid and semiarid regions of North Africa, the Middle East, and Patagonia (fig. S6). However, the models estimate a large range in the contribution of combustion aerosols to the deposition fluxes of total (from 2.6 to 7.1% on a global mean) and labile Fe (from

9 to 44% on a global mean) (Fig. 6). For total Fe, this range in estimates could be due to differences in the relative emission strengths of dust versus combustion-derived Fe (fig. S6), the mineralogical composition at the source region, the size distribution of airborne dust particles, and the meteorological data in the models (34). Because minerals in soils differ in their Fe content, spanning from 0.2 to 70%, Fe content in aerosols depends on the database of mineral composition in clay- and silt-sized soils, and the global mean Fe content in mineral dust emissions ranges from 2.6 to 3.5% (34).

The differences in the contribution of combustion aerosols to the total deposition fluxes among model results are significantly larger for labile Fe (22% for IMPACT, 44% for TM4-ECPL, and 9.3% for CAM4) than for total Fe (2.6% for IMPACT, 7.1% for TM4-ECPL, and 3.1% for CAM4) and increase with distance from the major dust source regions (Fig. 6). This is largely due to the differences in the assumed solubility of dust and combustion aerosols upon emission (table S1) and the subsequent enhancement of Fe solubility dynamically calculated from the simulated amount of atmospheric processing during transport. To show the sensitivity of simulated Fe solubility to atmospheric processing, the initial solubilities of 0.45% for dust and 4% for combustion aerosols (32) are prescribed with no atmospheric processing in Fig. 6 (C, F, and I). When atmospheric processing is not considered to enhance Fe solubility, the IMPACT model shows lower contribution of combustion aerosols than that with atmospheric processing over the remote ocean, because the faster dissolution schemes at lower pH than those at higher pH primarily work for wet combustion aerosols during atmospheric transport. The IMPACT model results are reasonably consistent with observations, which indicate much more increases in aerosol Fe solubilities over the open ocean from those near sources of biomass burning and coal combustion (24, 26, 43), compared to that for mineral dust during atmospheric transport (23, 42). When atmospheric processing is neglected, TM4-ECPL model shows higher contribution of combustion aerosols over the Southern Ocean, because simulated labile Fe over the ocean is due only to primary emissions (initial solubility) and labile Fe is removed faster than total Fe by wet deposition during atmospheric transport. Therefore, reducing uncertainties in model estimates of labile Fe deposition fluxes primarily requires improved parameterization for the factors that control aerosol Fe solubility (table S1) and the relative contribution of combustion aerosols to the labile fraction of aerosol Fe (Fig. 6).

CONCLUSIONS
The models need to consider the emissions of pyrogenic Fe-containing aerosols and their atmospheric transformation to simulate the high Fe solubility at low total aerosol Fe concentrations in the Northern Hemisphere. We found that the models did not reproduce the high Fe solubility over the Southern Ocean, suggesting potentially missing sources of pyrogenic Fe-containing aerosols and their dissolution processes. Further investigations of processes enhancing Fe solubility are needed in aerosols, rain (liquid cloud), and snow (ice cloud) over the oceans. A standard analytical method for assessing aerosol Fe solubility for polluted and clean environments is a high priority for future studies. Furthermore, our study suggests that assessments of atmospheric fluxes of labile Fe to the open oceans should consider Fe-containing aerosols emanating from both pyrogenic and lithogenic sources for accurately predicting anthropogenic perturbations to oceanic nutrient biogeochemistry.
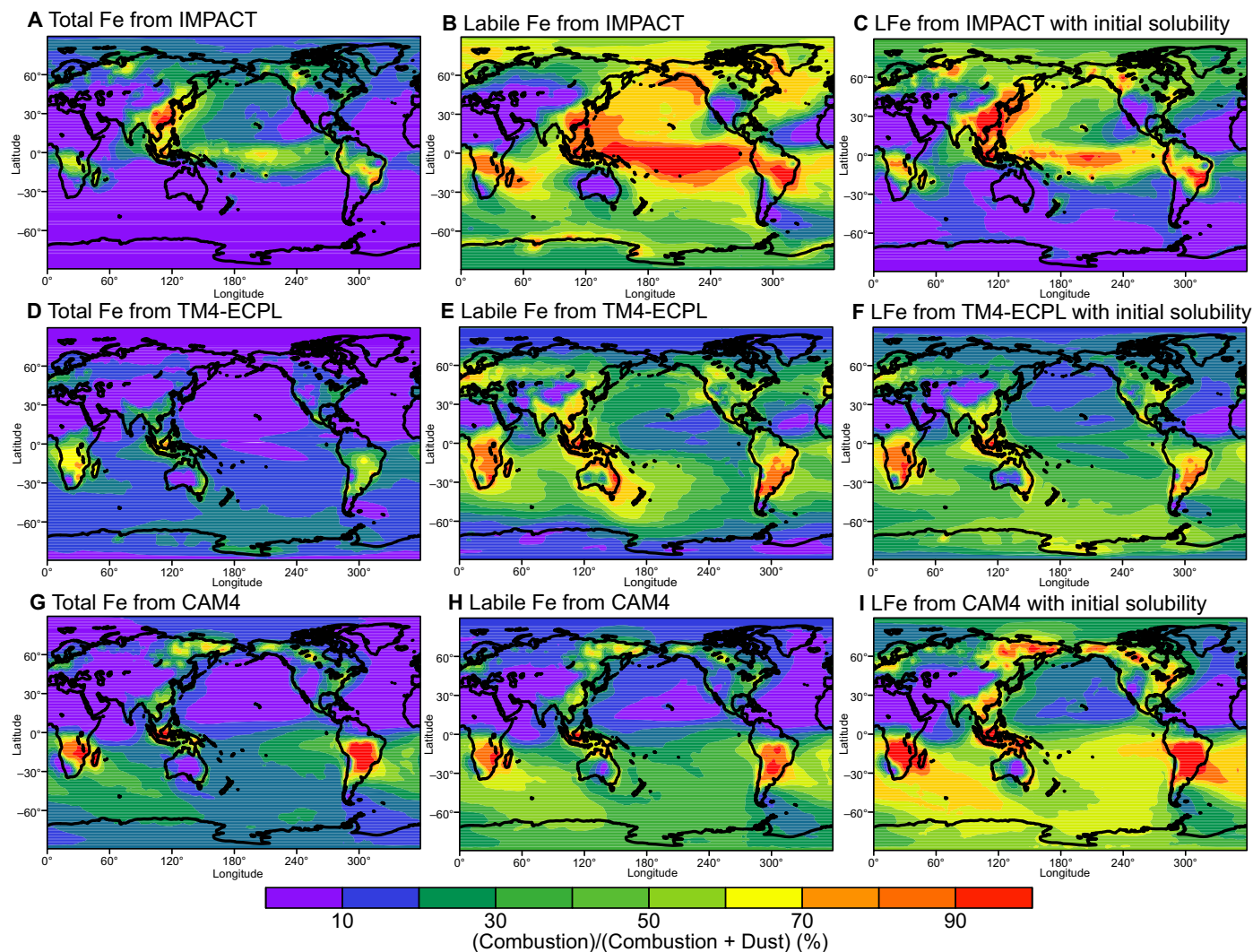
Fig. 6. Proportion of pyrogenic Fe in total aerosol Fe and labile Fe. Percentage of total aerosol Fe from combustion aerosols (**A**, **D**, and **G**) and the percentage of labile Fe from combustion aerosols to the total atmospheric Fe deposition flux (combustion and dust) calculated from three models with atmospheric processing (**B**, **E**, and **H**) and without atmospheric processing (**C**, **F**, and **I**).

MATERIALS AND METHODS
Global atmospheric models
The global atmospheric models used in this study are summarized in table S1 (*15*, *18*, *19*, *28*). The models participating in the intercomparison studies, within the framework of the GESAMP Working Group 38, differ in how the Fe emission and dissolution schemes are coupled and in the complexity of those schemes such as the inclusion or exclusion of combustion aerosols (*34*). Neither meteorological conditions nor emission inventories in these simulations were prescribed to a specific year. We bias-corrected the size-resolved mineral dust loading and deposition fluxes calculated by each model using recently obtained constraints on size-resolved dust loading (*34*, *51*).

Fe solubility from mineral dust in the four models (and for combustion aerosols in IMPACT and CAM4) increases with atmospheric processing. The amount of dissolved Fe is primarily determined by two factors: (i) content of labile Fe and (ii) dissolution rates of less labile Fe. Only a fraction of the less labile Fe can be dissolved during aerosol lifetimes in the atmosphere. Laboratory studies have de-

monstrated that the dissolution rate of Fe from minerals is strongly dependent on the proton concentration in bulk solution, the mineral surface concentration of oxalate, solar radiation, and the mineralogy (*16*, *20*, *27*, *30*). IMPACT, TM4-ECPL, and GEOS-Chem involved thermodynamic equilibrium modules to estimate the acidity in the aqueous phase of hygroscopic particles (*7*, *17*, *18*). On the other hand, CAM4 used two pH values (i.e., pH = 2 or pH = 7.5), which depended on the simulated ratio of calcite to sulfate (*13*). Note that coating of aerosols with inorganic and organic matter, and restructuring of the aggregates during the dispersion of the plume released by the combustion sources, is part of the so-called plume chemistry and is a sub–grid scale phenomenon in coarse-scale models. Thus, models that prescribed the Fe solubility for combustion aerosols at the emission level (table S1) implicitly assumed that atmospheric processing of aerosols also produced labile Fe within each grid box at the emission level. Therefore, the emissions treated in the models as primary sources also included secondary sources occurring within the large grid box, which could not be separated into primary emission

and rapid secondary formation in the atmosphere. The Fe solubilities were derived from the sum of mineral dust and combustion aerosols in IMPACT, TM4-ECPL, and CAM4, but only for mineral dust in GEOS-Chem.

Constraining estimates of Fe concentration

The daily averages of Fe concentration and solubility at the surface from four models were used for a comparison with the ambient measurements over the oceans (fig. S1 and table S2) (10, 21, 23, 24, 26, 37, 41–43, 49, 50, 52–59). When the field data uncertainties were not available, regional averages of relative SDs (SD divided by the average number of replicates) were used to estimate the SDs of the measurements. Mineral dust and biomass burning emissions are highly episodic and exhibit seasonal and interannual variability (5). It is, therefore, problematic to compare the monthly mean values of model estimates with the field data from different times of year, or different years. Moreover, the field observations have shown relatively high solubility at low concentration in aerosols influenced by combustion sources (24–26). Thus, aerosols at high atmospheric concentration can be more representative of mineral dust aerosols, while mixed aerosols from different sources, i.e., dust and combustion aerosols, may be more representative at low atmospheric concentration. This suggests that modeled Fe concentrations should be consistent with the measurements to assess the relative contribution of each source. However, direct association of model estimates to a specific cruise track and time period can introduce biases when used as a reference for larger regions and different time periods. The maximum likelihood method has been operationally implemented to atmospheric data assimilation systems to estimate the state of the atmosphere from observations and models. Therefore, the MLEs of Fe concentration, s_a, with error variance, σ_a^2, were derived from the measurements, s_o, and a priori daily estimates modeled in the same month as the measurements, s_b, with corresponding error variances, σ_o^2 and σ_b^2, respectively.

$$s_a = s_b + \frac{\sigma_b^2}{\sigma_o^2 + \sigma_b^2} \times (s_o - s_b) \quad (1)$$

$$\sigma_a^2 = \frac{\sigma_o^2 \sigma_b^2}{\sigma_o^2 + \sigma_b^2} \quad (2)$$

Using the probability function of the MLEs of Fe concentration assuming a normal distribution (MATLAB function), the weighted averages and SDs of Fe concentration and solubility were calculated. The a posteriori data were used as simulated estimates for the comparison with the measurements when MLEs of Fe concentration fell within $\pm 2\sigma_o$ of the measurements (fig. S1 and table S2).

Degree of atmospheric processing of Fe

Fe-containing aerosols from combustion sources are characterized by high solubility in solution (i.e., leaching media), compared to mineral dust, because the chemical form of Fe in the combustion aerosol may be inherently more labile (e.g., ferric sulfate and nanocrystals of Fe oxides). Because the aerosol water associated with combustion aerosols can be very acidic (pH generally below 3) (60) in the presence of enough organic ligands, Fe dissolution is significantly facilitated via proton-promoted, ligand-promoted, and photoreductive mechanisms,

and labile Fe is maintained in solution, resulting in relatively high solubility for combustion aerosols (27, 33). Therefore, the contribution of labile Fe to the sum of labile and less labile Fe may be viewed as the degree of atmospheric processing before deposition into the ocean. To assess the degree of atmospheric photochemical processing of Fe from the less labile forms, the ratio of Fe solubility estimates from two leaching methods (ultrahigh-purity water leach and 25% acetic acid leach) (23) was used according to the following equation

$$(\text{Degree of atmospheric processing of Fe}) = \frac{[\text{Fe}]_{\text{water leach}}}{[\text{Fe}]_{\text{water leach}} + [\text{Fe}]_{\text{acid leach}}} \quad (3)$$

The pH value of the 25% acetic acid leach (pH 2.1) is consistent with the pH estimates of water surrounding deliquescent aerosols using a thermodynamic equilibrium model at a rural location in the southeastern United States during 1998–2013 (60).

SUPPLEMENTARY MATERIALS

Supplementary material for this article is available at http://advances.sciencemag.org/cgi/content/full/5/5/eaau7671/DC1

Fig. S1. Fe solubility (%) of aerosols collected during multiple field campaigns for the field data and the simulated estimates from models used in this study.
Fig. S2. Comparison of simulated estimates and observed values for total Fe concentration (ng m^{-3}).
Fig. S3. Comparison of simulated estimates with combustion aerosols plus mineral dust and observed values for labile Fe concentration (ng m^{-3}).
Fig. S4. Comparison of simulated estimates with mineral dust only and observed values for labile Fe concentration (ng m^{-3}).
Fig. S5. Model estimates of Fe solubility in aerosols versus field data collected during multiple field campaigns (triangles for Arabian Sea and circles for others).
Fig. S6. Deposition fluxes of total Fe (ng Fe m^{-2} s^{-1}) from dust and combustion sources to present-day oceans.
Fig. S7. Deposition fluxes of labile Fe (ng Fe m^{-2} s^{-1}) from dust and combustion sources to present-day oceans.
Table S1. Summary of averaged Fe solubility in atmospheric models used in this study.
Table S2. Latitude, longitude, month, and Fe solubility (%) in aerosols for the intercomparison study.
Table S3. Comparison of Fe solubility (%) between the simulated estimates from models and field data.

REFERENCES AND NOTES

1. A. Tagliabue, A. R. Bowie, P. W. Boyd, K. N. Buck, K. S. Johnson, M. A. Saito, The integral role of iron in ocean biogeochemistry. Nature 543, 51–59 (2017).
2. T. D. Jickells, Z. S. An, K. K. Andersen, A. R. Baker, G. Bergametti, N. Brooks, J. J. Cao, P. W. Boyd, R. A. Duce, K. A. Hunter, H. Kawahata, N. Kubilay, J. laRoche, P. S. Liss, N. Mahowald, J. M. Prospero, A. J. Ridgwell, I. Tegen, R. Torres, Global iron connections between desert dust, ocean biogeochemistry, and climate. Science 308, 67–71 (2005).
3. G. Zhuang, Z. Yi, R. A. Duce, P. R. Brown, Link between iron and sulphur cycles suggested by detection of Fe(II) in remote marine aerosols. Nature 355, 537–539 (1992).
4. N. Meskhidze, W. L. Chameides, A. Nenes, Dust and pollution: A recipe for enhanced ocean fertilization? J. Geophys. Res. D Atmos. 110, 1–23 (2005).
5. N. M. Mahowald, S. Engelstaedter, C. Luo, A. Sealy, P. Artaxo, C. Benitez-Nelson, S. Bonnet, Y. Chen, P. Y. Chuang, D. D. Cohen, F. Dulac, B. Herut, A. M. Johansen, N. Kubilay, R. Losno, W. Maenhaut, A. Paytan, J. M. Prospero, L. M. Shank, R. L. Siefert, Atmospheric iron deposition: Global distribution, variability, and human perturbations. Annu. Rev. Mar. Sci. 1, 245–278 (2009).
6. A. R. Baker, O. Laskina, V. H. Grassian, Processing and ageing in the atmosphere, in Mineral Dust: A Key Player in the Earth System, P. Knippertz, J.-B. W. Stuut, Eds. (Springer, 2014), pp. 75–92.
7. N. Meskhidze, W. L. Chameides, A. Nenes, G. Chen, Iron mobilization in mineral dust: Can anthropogenic SO$_2$ emissions affect ocean productivity? Geophys. Res. Lett. 30, 2085 (2003).

8. M. Kanakidou, S. Myriokefalitakis, K. Tsigaridis, Aerosols in atmospheric chemistry and biogeochemical cycles of nutrients. *Environ. Res. Lett.* **13**, 063004 (2018).

9. N. Meskhidze, M. S. Johnson, D. Hurley, K. Dawson, Influence of measurement uncertainties on fractional solubility of iron in mineral aerosols over the oceans. *Aeolian Res.* **22**, 85–92 (2016).

10. E. R. Sholkovitz, P. N. Sedwick, T. M. Church, A. R. Baker, C. F. Powell, Fractional solubility of aerosol iron: Synthesis of a global-scale data set. *Geochim. Cosmochim. Acta* **89**, 173–189 (2012).

11. A. R. Baker, T. D. Jickells, Mineral particle size as a control on aerosol iron solubility. *Geophys. Res. Lett.* **33**, L17608 (2006).

12. Z. B. Shi, M. T. Woodhouse, K. S. Carslaw, M. D. Krom, G. W. Mann, A. R. Baker, I. Savov, G. R. Fones, B. Brooks, N. Drake, T. D. Jickells, L. G. Benning, Minor effect of physical size sorting on iron solubility of transported mineral dust. *Atmos. Chem. Phys.* **11**, 8459–8469 (2011).

13. C. Luo, N. M. Mahowald, N. Meskhidze, Y. Chen, R. L. Siefert, A. R. Baker, A. M. Johansen, Estimation of iron solubility from observations and a global aerosol model. *J. Geophys. Res. Atmos.* **110**, D23307 (2005).

14. A. Ito, Y. Feng, Role of dust alkalinity in acid mobilization of iron. *Atmos. Chem. Phys.* **10**, 9237–9250 (2010).

15. M. S. Johnson, N. Meskhidze, Atmospheric dissolved iron deposition to the global oceans: Effects of oxalate-promoted Fe dissolution, photochemical redox cycling, and dust mineralogy. *Geosci. Model Dev.* **6**, 1137–1155 (2013).

16. Z. Shi, S. Bonneville, M. D. Krom, K. S. Carslaw, T. D. Jickells, A. R. Baker, L. G. Benning, Iron dissolution kinetics of mineral dust at low pH during simulated atmospheric processing. *Atmos. Chem. Phys.* **11**, 995–1007 (2011).

17. A. Ito, L. Xu, Response of acid mobilization of iron-containing mineral dust to improvement of air quality projected in the future. *Atmos. Chem. Phys.* **14**, 3441–3459 (2014).

18. S. Myriokefalitakis, N. Daskalakis, N. Mihalopoulos, A. R. Baker, A. Nenes, M. Kanakidou, Changes in dissolved iron deposition to the oceans driven by human activity: A 3-D global modelling study. *Biogeosciences* **12**, 3973–3992 (2015).

19. R. A. Scanza, D. S. Hamilton, C. P. Garcia-Pando, C. Buck, A. Baker, N. M. Mahowald, Atmospheric processing of iron in mineral and combustion aerosols: Development of an intermediate-complexity mechanism suitable for Earth system models. *Atmos. Chem. Phys.* **18**, 14175–14196 (2018).

20. A. Ito, Z. Shi, Delivery of anthropogenic bioavailable iron from mineral dust and combustion aerosols to the ocean. *Atmos. Chem. Phys.* **16**, 85–99 (2016).

21. C. S. Buck, W. M. Landing, J. A. Resing, G. T. Lebon, Aerosol iron and aluminum solubility in the northwest Pacific Ocean: Results from the 2002 IOC cruise. *Geochem. Geophys. Geosyst.* **7**, Q04M07 (2006).

22. C. J. M. Berger, S. M. Lippiatt, M. G. Lawrence, K. W. Bruland, Application of a chemical leach technique for estimating labile particulate aluminum, iron, and manganese in the Columbia River plume and coastal waters off Oregon and Washington. *J. Geophys. Res.* **113**, C00B01 (2008).

23. R. U. Shelley, W. M. Landing, S. J. Ussher, H. Planquette, G. Sarthou, Regional trends in the fractional solubility of Fe and other metals from North Atlantic aerosols (GEOTRACES cruises GA01 and GA03) following a two-stage leach. *Biogeosciences* **15**, 2271–2288 (2018).

24. C. Guieu, S. Bonnet, T. Wagener, M.-D. Loÿe-Pilot, Biomass burning as a source of dissolved iron to the open ocean? *Geophys. Res. Lett.* **32**, L19608 (2005).

25. P. N. Sedwick, E. R. Sholkovitz, T. M. Church, Impact of anthropogenic combustion emissions on the fractional solubility of aerosol iron: Evidence from the Sargasso Sea. *Geochem. Geophys. Geosyst.* **8**, Q10Q06 (2007).

26. S. Bikkina, M. M. Sarin, A. Kumar, Impact of anthropogenic sources on aerosol iron solubility over the Bay of Bengal and the Arabian Sea. *Biogeochemistry* **110**, 257–268 (2012).

27. H. Chen, V. H. Grassian, Iron dissolution of dust source materials during simulated acidic processing: The effect of sulfuric, acetic, and oxalic acids. *Environ. Sci. Technol.* **47**, 10312–10321 (2013).

28. A. Ito, G. Lin, J. E. Penner, Radiative forcing by light-absorbing aerosols of pyrogenic iron oxides. *Sci. Rep.* **8**, 7347 (2018).

29. A. W. Schroth, J. Crusius, E. R. Sholkovitz, B. C. Bostick, Iron solubility driven by speciation in dust sources to the ocean. *Nat. Geosci.* **2**, 337–340 (2009).

30. H. Fu, J. Lin, G. Shang, W. Dong, V. H. Grassian, G. R. Carmichael, Y. Li, J. Chen, Solubility of iron from combustion source particles in acidic media linked to iron speciation. *Environ. Sci. Technol.* **46**, 11119–11127 (2012).

31. O. Sippula, J. Hokkinen, H. Puustinen, P. Yli-Pirilä, J. Jokiniemi, Comparison of particle emissions from small heavy fuel oil and wood-fired boilers. *Atmos. Environ.* **43**, 4855–4864 (2009).

32. C. Luo, N. Mahowald, T. Bond, P. Y. Chuang, P. Artaxo, R. Siefer, Y. Chen, J. Schauer, Combustion iron distribution and deposition. *Global Biogeochem. Cycles* **22**, GB1012 (2008).

33. A. Ito, Atmospheric processing of combustion aerosols as a source of bioavailable iron. *Environ. Sci. Technol. Lett.* **2**, 70–75 (2015).

34. S. Myriokefalitakis, A. Ito, M. Kanakidou, A. Nenes, M. C. Krol, N. M. Mahowald, R. A. Scanza, D. S. Hamilton, M. S. Johnson, N. Meskhidze, J. F. Kok, C. Guieu, A. R. Baker, T. D. Jickells, M. M. Sarin, S. Bikkina, R. Shelley, A. Bowie, M. M. G. Perron, R. A. Duce, The GESAMP atmospheric iron deposition model intercomparison study. *Biogeosciences* **15**, 6659–6684 (2018).

35. A. Ito, Global modeling study of potentially bioavailable iron input from shipboard aerosol sources to the ocean. *Global Biogeochem. Cycles* **27**, 1–10 (2013).

36. K. V. Desboeufs, A. Sofikitis, R. Losno, J. L. Colin, P. Ausset, Dissolution and solubility of trace metals from natural and anthropogenic aerosol particulate matter. *Chemosphere* **58**, 195–203 (2005).

37. A. Kumar, M. M. Sarin, S. Bikkina, Aerosol iron solubility over Bay of Bengal: Role of anthropogenic sources and chemical processing. *Mar. Chem.* **121**, 167–175 (2010).

38. S. Bikkina, M. M. Sarin, Atmospheric dry-deposition of mineral dust and anthropogenic trace metals to the Bay of Bengal. *J. Mar. Syst.* **126**, 56–68 (2013).

39. A. M. Johansen, M. R. Hoffmann, Chemical characterization of ambient aerosol collected during the northeast monsoon season over the Arabian Sea: Anions and cations. *J. Geophys. Res. Atmos.* **109**, D05305 (2004).

40. R. L. Siefert, A. M. Johansen, M. R. Hoffmann, Chemical characterization of ambient aerosol collected during the southwest monsoon and intermonsoon seasons over the Arabian Sea: Labile-Fe(II) and other trace metals. *J. Geophys. Res. Atmos.* **104**, 3511–3526 (1999).

41. A. R. Baker, C. Adams, T. G. Bell, T. D. Jickells, L. Ganzeveld, Estimation of atmospheric nutrient inputs to the Atlantic Ocean from 50°N to 50°S based on large-scale field sampling: Iron and other dust-associated elements. *Global Biogeochem. Cycles* **27**, 755–767 (2013).

42. A. R. Baker, M. French, K. L. Linge, Trends in aerosol nutrient solubility along a west–east transect of the Saharan dust plume. *Geophys. Res. Lett.* **33**, L07805 (2006).

43. A. R. Bowie, D. Lannuzel, T. A. Remenyi, T. Wagener, P. J. Lam, P. W. Boyd, C. Guieu, A. T. Townsend, T. W. Trull, Biogeochemical iron budgets of the Southern Ocean south of Australia: Decoupling of iron and nutrient cycles in the subantarctic zone by the summertime supply. *Global Biogeochem. Cycles* **23**, GB4034 (2009).

44. A. Ito, J. F. Kok, Do dust emissions from sparsely vegetated regions dominate atmospheric iron supply to the Southern Ocean? *J. Geophys. Res.* **122**, 3987–4002 (2017).

45. H. Matsui, N. M. Mahowald, N. Moteki, D. S. Hamilton, S. Ohata, A. Yoshida, M. Koike, R. A. Scanza, M. G. Flanner, Anthropogenic combustion iron as a complex climate forcer. *Nat. Commun.* **9**, 1593 (2018).

46. K. Kim, W. Choi, M. R. Hoffmann, H.-I. Yoon, B.-K. Park, Photoreductive dissolution of iron oxides trapped in ice and its environmental implications. *Environ. Sci. Technol.* **44**, 4142–4148 (2010).

47. V. H. L. Winton, R. Edwards, B. Delmonte, A. Ellis, P. S. Andersson, A. Bowie, N. A. N. Bertler, P. Neff, A. Tuohy, Multiple sources of soluble atmospheric iron to Antarctic waters. *Global Biogeochem. Cycles* **30**, 421–437 (2016).

48. M. Kurisu, Y. Takahashi, T. Iizuka, M. Uematsu, Very low isotope ratio of iron in fine aerosols related to its contribution to the surface ocean. *J. Geophys. Res. Atmos.* **121**, 11119–11136 (2016).

49. C. S. Buck, W. M. Landing, J. Resing, Pacific Ocean aerosols: Deposition and solubility of iron, aluminum, and other trace elements. *Mar. Chem.* **157**, 117–130 (2013).

50. Y. Gao, G. Xu, J. Zhan, J. Zhang, W. Li, Q. Lin, L. Chen, H. Lin, Spatial and particle size distributions of atmospheric dissolvable iron in aerosols and its input to the Southern Ocean and coastal East Antarctica. *J. Geophys. Res. Atmos.* **118**, 12634–12648 (2013).

51. J. F. Kok, D. A. Ridley, Q. Zhou, R. L. Miller, C. Zhao, C. L. Heald, D. S. Ward, S. Albani, K. Haustein, Smaller desert dust cooling effect estimated from analysis of dust size and abundance. *Nat. Geosci.* **10**, 274–278 (2017).

52. C. S. Buck, W. M. Landing, J. A. Resing, Particle size and aerosol iron solubility: A high-resolution analysis of Atlantic aerosols. *Mar. Chem.* **120**, 14–24 (2010).

53. C. S. Buck, A. N. A. Aguilar-Islas, C. Marsay, D. Kadko, W. M. Landing, Trace element concentrations, elemental ratios, and enrichment factors observed in aerosol samples collected during the US GEOTRACES eastern Pacific Ocean transect (GP16). *Chem. Geol.* **511**, 212–224 (2019).

54. T. D. Jickells, A. R. Baker, R. Chance, Atmospheric transport of trace elements and nutrients to the oceans. *Philos. Trans. A Math. Phys. Eng. Sci.* **374**, 20150286 (2016).

55. C. Guieu, S. Bonnet, A. Petrenko, C. Menkes, V. Chavagnac, K. Desboeufs, C. Maes, T. Moutin, Iron from a submarine source impacts the productive layer of the Western Tropical South Pacific (WTSP). *Sci. Rep.* **8**, 9075 (2018).

56. C. F. Powell, A. R. Baker, T. D. Jickells, H. W. Bange, R. J. Chance, C. Yodle, Estimation of the atmospheric flux of nutrients and trace metals to the eastern Tropical North Atlantic Ocean. *J. Atmos. Sci.* **72**, 4029–4045 (2015).

57. E. P. Achterberg, S. Steigenberger, C. M. Marsay, F. A. C. Lemoigne, S. C. Painter, A. R. Baker, D. P. Connelly, C. M. Moore, A. Tagliabue, T. Tanhua, Iron biogeochemistry in the high latitude North Atlantic Ocean. *Sci. Rep.* **8**, 1283 (2018).

58. A. F. Longo, Y. Feng, B. Lai, W. M. Landing, R. U. Shelley, A. Nenes, N. Mihalopoulos,
     K. Violaki, E. D. Ingall, Influence of atmospheric processes on the solubility and
     composition of iron in Saharan dust. *Environ. Sci. Technol.* **50**, 6912–6920 (2016).
59. T. Wagener, "Le fer à l'interface océan-atmosphère: Flux et processus de dissolution dans
     l'eau de mer," thesis, Université de la Méditerranée-Aix-Marseille II (2008).
60. R. J. Weber, H. Guo, A. G. Russell, A. Nenes, High aerosol acidity despite declining
     atmospheric sulfate concentrations over the past 15 years. *Nat. Geosci.* **9**, 282–285
     (2016).

Citation: A. Ito, S. Myriokefalitakis, M. Kanakidou, N. M. Mahowald, R. A. Scanza, D. S. Hamilton,
A. R. Baker, T. Jickells, M. Sarin, S. Bikkina, Y. Gao, R. U. Shelley, C. S. Buck, W. M. Landing,
A. R. Bowie, M. M. G. Perron, C. Guieu, N. Meskhidze, M. S. Johnson, Y. Feng, J. F. Kok, A. Nenes,
R. A. Duce, Pyrogenic iron: The missing link to high iron solubility in aerosols. *Sci. Adv.* **5**,
eaau7671 (2019).